Environmental Science & Technology

pubs.acs.org/est

Article

Impact of Organic Matter on Microbially-Mediated Reduction and Mobilization of Arsenic and Iron in Arsenic(V)-Bearing Ferrihydrite

Xiaolin Cai, Laurel K. ThomasArrigo,* Xu Fang, Sylvain Bouchet, Yanshan Cui,* and Ruben Kretzschmar

Cite This: *Environ. Sci. Technol.* 2021, 55, 1319−1328

Read Online

ACCESS | Metrics & More | Article Recommendations | Supporting Information

ABSTRACT: Under anoxic conditions, the interactions between As-bearing ferrihydrite (Fh) and As(V)-reducing bacteria are known to cause Fh transformations and As mobilization. However, the impact of different types of organic matter (OM) on microbial As/Fe transformation in As-bearing Fh-organic associations remains unclear. In our study, we therefore exposed arsenate-adsorbed ferrihydrite, ferrihydrite-PGA (polygalacturonic acid), and ferrihydrite-HA (humic acid) complexes to two typical Fe(III)- and As(V)-reducing bacteria, and followed the fate of Fe and As in the solid and aqueous phases. Results show that PGA and HA promoted the reductive dissolution of Fh, resulting in 0.7−1.6 and 0.8−1.9 times more As release than in the OM-free Fh, respectively. This was achieved by higher cell numbers in the presence of PGA, and through Fe-reduction via electron-shuttling facilitated by HA. Arsenic-XAS results showed that the solid-phase arsenite fraction in Fh-PGA and Fh-HA was 15−19% and 27−28% higher than in pure Fh, respectively. The solid-associated arsenite fraction likely increased because PGA promoted cell growth and As(V) reduction, while HA provided electron shuttling compounds for direct microbial As(V)-reduction. Collectively, our findings demonstrate that As speciation and partitioning during microbial reduction of Fh-organic associations are strongly influenced by PGA and HA, as well as the strains' abilities to utilize electron-shuttling compounds.

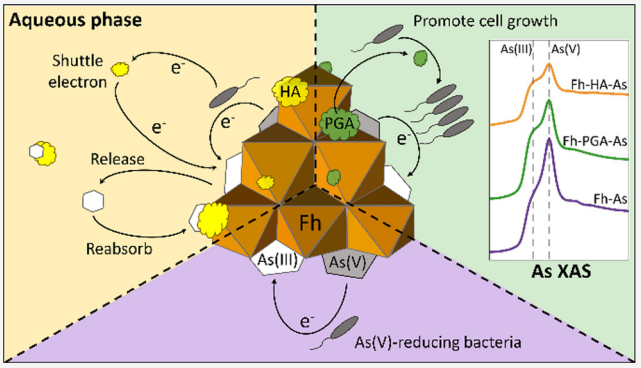

INTRODUCTION

Arsenic (As) is a highly toxic and carcinogenic metalloid that adversely impacts human health globally. Since the toxicity, mobility, and bioavailability of As depends on its chemical speciation, biogeochemical transformations of As and its partitioning between solid and aqueous phases have motivated many studies over the past decade. Previous investigations showed that in soils and sediments, arsenic is primarily associated with poorly crystalline Fe(III)-(oxyhydr)oxides, such as ferrihydrite (Fh).[1,2] The fate of Fe(III)-(oxyhydr)-oxide-bound As is generally regulated by dissimilatory Fe(III) and As(V) reduction and sequestration by the newly forming secondary minerals.[3−7] In nature, however, Fe(III)-(oxyhydr)-oxides often coexist with natural organic matter (OM), resulting in the formation of organic-mineral coprecipitates and adsorption complexes.[8−12] Coprecipitation or adsorption of organic matter can alter the physical and chemical properties of Fe(III)-(oxyhydr)oxides[13] and may consequently influence microbially mediated Fe/As mobilization.[14,15] For example, the associated OM may block the interparticle pores of minerals and induce aggregation of Fe(III)-(oxyhydr)oxides,[13] or influence mineral structure,[16] thus decelerating microbial Fe reduction.[17,18] In contrast, quinone groups found in humic acids may provide redox active electron-shuttling compounds for reducing microorganisms to facilitate dissimilatory Fe(III)-reduction of organic-mineral associations[19−21] or complex with dissolved Fe(II,III), thereby promoting Fe reduction and solubilization.[22,23] Furthermore, cell derived organic matter may enhance As release from biogenic Fe(III)-(oxyhydr)oxides by reversing the surface charge of Fe minerals from positive to negative, competing with As(V) for sorption sites, or forming dissolved complexes with As(III).[6] And, in a recent study, the presence of humic acid was shown to hinder Fe-mineral transformations and result in higher As(V) release due to less structural incorporation of As(V) into (secondary) Fe-minerals.[24] However, the influence of different types of organic matter on As speciation changes and the reductive mobilization of Fe(III)-(oxyhydr)oxide-associated As by As-

Received: August 8, 2020
Revised: November 16, 2020
Accepted: December 9, 2020
Published: December 30, 2020

https://dx.doi.org/10.1021/acs.est.0c05329
Environ. Sci. Technol. 2021, 55, 1319−1328

(V)-reducing bacteria, as well as the mechanisms through which this is accomplished, remain unclear.

Previous studies investigating the effect of OM on microbially mediated As and Fe mobilization often preferred the utilization of electron-shuttling compounds such as humic acid and anthraquinone-2,6-disulfonic acid (AQDS).[18,25,26] Widespread organic matter in nature, however, is not restricted to these types of compounds. As an important part of plant root exudates or extracellular polymeric substances (EPS) of microorganisms, polysaccharides have also been documented to be commonly associated with Fe(III)-(oxyhydr)oxides in freshwater and soil[27,28] and are known to strongly inhibit kinetic Fe(II)-catalyzed mineral transformations,[29,30] which may indirectly influence the mobilization of Fe(III)-(oxyhydr)-oxides-bound As. Alternatively, some polysaccharides have been shown to provide carbon sources for a wide variety of microorganisms,[31,32] suggesting that these polysaccharides may impact microbially mediated As transformation by influencing microbial growth.

In addition to organic matter, the reduction and dissolution of Fe-minerals could also be controlled by the types of bacteria. Poggenburg et al.[12] incubated diverse Fe-organic associations with two different dissimilatory Fe(III)-reducing bacteria, and reported that Fe reduction by *Shewanella putrefaciens* depended on the content of usable electron-shuttling compounds, whereas Fe reduction by *Geobacter metallireducens* was determined by the aggregation degree of Fe-oxides particles. These results suggest that As(V)-reducing bacteria from different species may also have a diverging effect on the mobilization and transformation of solid-phase associated As. Organisms like *Shewanella* have been used in numerous studies regarding microbial Fe and As reduction. But there are many other microorganisms in the environment that can reduce Fe(III) and As(V). Recently, two As(V)-reducing bacteria, *Desulfitobacterium* sp. DJ-3 and *Exiguobacterium* sp. DJ-4, were isolated from the soil of an arsenic-contaminated mine in Inner Mongolia, China.[33] Strains DJ-3 and DJ-4 can utilize Fe(III) and As(V) as electron acceptors.[33,34] Among these strains, DJ-4 is the first *Exiguobacterium* strain isolated from soil that is capable of reducing As(V).[33] *Desulfitobacterium* is known as a versatile bacterial genus capable of using a wide variety of electron acceptors and carbon sources.[35,36] Specifically, previous studies found that the abundance of *Desulfitobacterium* may increase significantly at high electron-shuttling compound levels,[26] and the reduction and mobilization of As is likely to be mainly mediated by *Desulfitobacterium* under this condition.[37] In the current study, we therefore utilized these two typical As(V)-reducing bacteria to elucidate the impact of different OM on the microbial Fe and As mobilization and transformation of As-bearing Fe(III)-(oxyhydr)oxides.

To this end, we incubated the As(V)-reducing bacterial strains with As-bearing pure ferrihydrite and As-bearing ferrihydrite-organic adsorption complexes comprising different adsorbed OM: specifically, we used humic acid (HA, a typical organic matter providing redox active electron-shuttling compounds for reducing microorganisms) and polygalacturonic acid (PGA, a model compound for plant and microbial exopolysaccharides with no electron-shuttling ability).[38] Our study aimed to (1) investigate the impact of adsorbed HA and PGA and different bacterial species on the reductive dissolution of Fh and secondary mineral formation, and to (2) elucidate the mobilization and transformation of adsorbed As in mineral-organic adsorption complexes in the presence of different As(V)-reducing bacteria.

MATERIALS AND METHODS

Materials. All chemicals used were of reagent grade. All solutions were prepared from doubly deionized (DDI) water (18.2 MΩ·cm, Milli-Q, Millipore). Pahokee peat humic acid (Pahokee peat HA, 1S103H) was purchased from the International Humic Substances Society. Polygalacturonic acid (PGA, $(C_6H_8O_6)_n$, ≥ 90% (enzym.), M_w = 25−50 kDa) was purchased from Sigma-Aldrich. Detailed information about Pahokee peat HA and PGA is shown in Tables S1 and S2 and Figure S1 of the Supporting Information (SI).

Preparation of Fh and Adsorption Complexes. Poorly crystalline synthetic ferrihydrite (Fh) was prepared according to Schwertmann and Cornell,[39] with slight modifications. Briefly, 10 M NaOH was added dropwise to 1L of ferric chloride solution (0.4 M $FeCl_3{\cdot}6H_2O$) under vigorous stirring (1000/min) to a pH of 7.0 ± 0.1. The resulting dark brown precipitate suspension was left in a closed polyethylene flask at room temperature for 24 h, followed by centrifugation at 3500*g* for 20 min and repeated washing with DDI water until the electric conductivity in the supernatant was ≤10 μS/cm. To prepare adsorption complexes, 1 g of OM (PGA or HA) was resuspended in 1 L DDI water and the pH was subsequently adjusted to 7.0 using 1 M NaOH. The solutions were equilibrated overnight in darkness under vigorous stirring (1000/min). The synthetic ferrihydrite (50 g, moisture content: ∼84%) was then added to each OM solution and stirred (1000/min) for another 24 h in the dark to let the OM adsorb onto the mineral. The suspension was then centrifuged and washed as described in the synthesis of ferrihydrite. The Fh-OM adsorption complexes are hereafter referred to as Fh-PGA and Fh-HA (target C:Fe molar ratio is 0.39 and 0.59 for Fh-PGA and Fh-HA, respectively).

To prepare As(V)-adsorbed complexes, Fh, Fh-PGA and Fh-HA (containing ∼100 mmol of Fe(III)) were added to 300 mL of $Na_2HAsO_4{\cdot}7H_2O$ solution (4 mM) with pH adjusted to 7.0. The suspensions were then stirred for 24 h (target molar ratio of As:Fe was approximately 1:85) followed by centrifugation and washing steps as described above. Afterward, all synthesized precipitates were shock-frozen in liquid nitrogen,[40] freeze-dried, manually homogenized, and stored in brown glass in a desiccator until use. The As(V)-adsorbed Fh, Fh-PGA, and Fh-HA are hereafter named Fh-As, Fh-PGA-As, and Fh-HA-As, respectively.

Bacterial Strains and Microbial Incubation Experiments. To investigate the role of organic matter coatings on microbial Fe(III) and As(V) reduction and mobilization, Fh-As, Fh-PGA-As, and Fh-HA-As were respectively inoculated with *Desulfitobacterium* sp. DJ-3 and *Exiguobacterium* sp. DJ-4 for 18 days. The experiment was conducted in triplicate in an anoxic glovebox (<1 ppm (v/v) O_2). All solutions used were prepared from anoxic DDI water. The bacteria were grown to late-log phase in a minimal salt medium (MSM, preparation detailed in the SI, Table S3) which also contained 5 mM As(V). The cultures were then centrifuged at 8000*g* for 3 min to harvest the cells. After washing three times with 0.8% sterile NaCl, the cells were resuspended in MSM (without As(V)) adjusted to pH 7.3.

For the microbial incubation experiments, 0.2 g of Fh-As, Fh-PGA-As, and Fh-HA-As materials were weighed into 100 mL serum bottles. 50 mL of the bacterial suspension were

https://dx.doi.org/10.1021/acs.est.0c05329
Environ. Sci. Technol. 2021, 55, 1319−1328

Table 1. Elementary Composition, Specific Surface Area, And Pore Characteristics of Ferrihydrite and Adsorption Complexes

	content of						
initial samples	C[a] (mg/g)	Fe[a] (mg/g)	As[a] (mg/g)	molar C/Fe ratio	molar As/Fe ratio (*10^{-3})	SSA^{corr} (m^2/g)	average pore size (nm)
Fh-As	3.2 ± 0.1	552.8 ± 18.7	6.6 ± 0.3	0.03	9.0	305	3.7
Fh-PGA-As	34.7 ± 1.5	508.9 ± 5.0	6.3 ± 0.0	0.32	9.3	269	5.2
Fh-HA-As	48.8 ± 0.0	484.1 ± 15.2	5.6 ± 0.2	0.47	8.6	288	4.5

[a]Determined in triplicates. Specific surface areas measured were corrected for OM contents to obtain the N_2-accessible specific surface area of the mineral: SSA^{corr} = SSA/(1-OM), SSA denotes measured specific surface area (m^2/g) values, OM (g/g) refers to the organic matter content in the initial As(V)-adsorbed Fh and Fh-OM complexes. This was calculated based on the C-content of the organic matter (Tables S1 and S2).[13]

added to the serum bottles, which were then capped with butyl rubber stoppers and secured with aluminum-crimped caps. Control setups (without bacteria cells) were carried out in parallel to discount the effect of culture medium. The bottles were then placed on a horizontal shaker in the dark at 150 rpm at 37 °C and sampled periodically for further analyses.

To verify the individual role of PGA and HA on bacterial growth and microbial As transformation, additional experiments were conducted in which inoculated reaction bottles, like those described above, were supplemented with an additional spike of PGA or HA. Specifically, as described in the experimental setup above, Fh-As, Fh-PGA-As, and Fh-HA-As samples (0.2 g) were inoculated with strain DJ-3 in 50 mL of MSM. An additional 10 mg of PGA or HA was added at the time of inoculation, and the pH was subsequently adjusted to 7.3 using 1 M NaOH. The bottles were then crimp-sealed, stored on a horizontal shaker (150 rpm) in the dark, and sampled at 3 days for cell counting and at 18 days for aqueous-phase analyses.

Aqueous-Phase Analyses. Aqueous samples (3 mL) were taken anoxically in the glovebox directly prior to the addition of As(V)-adsorbed Fh and Fh-OM complexes (time point 0), and at 1, 3, 6, 9, and 18 days. Samples were passed through 0.22-μm nylon filters and acidified with HCl. Concentrations of total aqueous Fe and As were analyzed using inductively coupled plasma mass spectrometry (ICP-MS, 8800, Agilent). Arsenic species (As(III), As(V)) were separated and quantified by HPLC-ICP-MS (Agilent Technologies 1290 quaternary pump coupled to an ICP-QQQ 8800) using an anion-exchange column (Hamilton PRP-X100, 125 × 4.0 mm^2, 10 μm with the appropriate guard column) and a gradient elution using malonic acid as mobile phase (pH 5.6, from 1.3 to 9.3 mM in 3 min) adapted from Raber and co-workers.[41] Detailed instrumental parameters are provided in the SI.

Aqueous Fe speciation was determined using the colorimetric 1,10-phenanthroline method,[42] whereby the concentration of aqueous Fe(III) was determined from the difference between total Fe and Fe(II). The pH of the suspension was measured at each time point using a portable pH meter and the changes were less than 0.32 in all treatments during the incubation (Table S4). The impact of such small pH changes on As mobilization are expected to be negligible. The OM fraction that is easily desorbable from Fh was measured according to the method of Poggenburg and co-workers.[12] The adsorption complexes were resuspended in MSM (4 g/L) but without the addition of organic substances. After equilibration for 24 h on a horizontal shaker at 37 °C, the suspensions were filtered <0.45 μm and analyzed for organic carbon (OC) content with a Dimatoc 2000 TOC analyzer (Dimatec).[12]

Solid-Phase Sampling and Characterization. Suspensions (15 mL) were sampled in an anoxic glovebox at 6 and 18 days for solid-phase analysis. Solid samples were collected on 0.45-μm cellulose filters, thoroughly rinsed with DDI water, covered, and dried in the glovebox. Triplicate samples were combined, manually homogenized, and stored anoxically in darkness until further analysis.

To determine Fe and As contents in the (un)reacted Fh-As, Fh-PGA-As, and Fh-HA-As, ~ 2 mg of (un)reacted samples were dissolved in 1 mL of 30% HCl (Ultrapur, Merck). Since humic acids precipitate under acidic conditions, dissolution with 30% HCl may only dissolve Fe-mineral-associated As in Fh-HA-As. The incubated Fh-HA-As was therefore additionally digested with microwave digestion (Mars 6, CEM) to dissolve HA-associated As in addition to Fe-mineral associated As. Total Fe and As concentrations were measured using inductively coupled plasma optical emission spectrometry (ICP-OES, Agilent 5100 or Perkin Elmer Optima 7300V) after digestion. Carbon contents of the solid samples were analyzed with an elemental analyzer (CHNS-932, LECO). The functional groups of the OM fraction were characterized by Fourier-transform infrared (FT−IR) spectroscopy in attenuated total reflectance (ATR) mode. Details to ATR−FTIR analysis are provided in SI. The mineralogy of the (un)reacted Fh-As, Fh-PGA-As, and Fh-HA-As samples was characterized by X-ray diffraction (XRD, D8 Advance, Bruker). The mineralogical morphologies of the initial materials were studied with transmission electron microscopy (TEM, JEM-1200EX, JEOL). The specific surface area (SSA) of the samples was determined from the relative pressure range of 0.05−0.3 by the BET equation using a physisorption analyzer (ASAP2460, Micromeritics).[43] Pore size (adsorption average pore diameter) was determined via the Barrett−Joyner−Halenda (BJH) method.[44]

Synchrotron Measurements. To determine the speciation changes of Fe and As in the solid samples after incubating with As(V)-reducing bacteria, (un)reacted Fh-As, Fh-PGA-As, and Fh-HA-As samples were analyzed by Fe and As K-edge (7112 and 11 867 eV, respectively) X-ray absorption spectroscopy (XAS). For Fe, extended X-ray absorption fine structure (EXAFS) and X-ray absorption near the edge structure (XANES) spectra were collected in transmission mode at the XAFS beamline at the Elettra Synchrotron Light Source (ELETTRA, Trieste, Italy) and beamline 1W2B at the Beijing Synchrotron Radiation Facility (BSRF, Beijing, China). Arsenic K-edge XANES spectra were collected in fluorescence mode on beamline 14W at the Shanghai Synchrotron Radiation Facility (SSRF, Shanghai, China) using a solid-state Ge detector. Details to sample preparation, measurements, and analyses are provided in the SI.

Spectral data processing was performed in Athena.[45] All XAS spectra of Fe and As were normalized, background-subtracted, and least-squares fitted by a linear combination of appropriate reference materials spectra. For Fe, principal component

https://dx.doi.org/10.1021/acs.est.0c05329
Environ. Sci. Technol. 2021, 55, 1319−1328

analysis and target-transform testing (PCA-TT) was employed to select suitable references for linear combination fitting (LCF) using SixPack.[46] Details to PCA-TT, including references and results, are found in the SI. Linear combination fit analyses of k^3-weighted Fe EXAFS spectra were performed over a k-range of 2−10 Å^{-1}, and LCF analyses of k^3-weighted As XANES spectra were conducted over an energy range of −20 to 80 eV.

RESULTS AND DISCUSSION

Characterization of Initial As(V)-Adsorbed Fh and Fh-OM Complexes. The elemental composition of the initial Fh-As, Fh-PGA-As, and Fh-HA-As materials is presented in Table 1. Fe and As contents ranged from 484 to 553 and 5.6 to 6.6 mg/g, respectively. The molar ratio of As/Fe was 8.6−9.3 × 10^{-3}, which is consistent with the As/Fe molar ratios of As-contaminated soil samples collected in natural environment.[47] The molar ratio of C/Fe was 0.32−0.47; C contents were higher in Fh-HA-As (48.8 mg/g) than in Fh-PGA-As (34.7 mg/g) owing to the higher C content of HA (Tables S1 and S2). The specific surface areas and average pore sizes of the initial materials ranged from 269 to 305 m^2/g and 3.7 to 5.2 nm, respectively (Table 1). The SSA of Fh-PGA-As was the lowest, while the pore size of Fh-PGA-As was larger than Fh-As, which indicates that PGA may block the interparticle pores of Fh and, in addition, promote particle aggregation.[48,49] In the transmission electron microscopy images (Figure 1), fewer primary particles within the aggregate structure could be distinguished in Fh-PGA-As compared with Fh-As and Fh-HA-As materials, in agreement with the promoted aggregation of Fh particles by PGA.[13]

X-ray diffraction patterns of the initial materials are all identical (Figure S4), and confirm that all samples consisted of 6-line Fh, similarly described by Schwertmann et al.[50] The ATR−FTIR spectra of the initial materials show that organic functional groups of Fh-HA-As are dominated by deprotonated carboxylic groups, carbonyl groups, and alkanes, while Fh-PGA-As are dominated by deprotonated carboxylic groups, phenols, and ethers (Figure S8).

Effects of OM on Microbial Reductive Dissolution of Ferrihydrite. Aqueous Fe (Fe_{aq}) concentrations and speciation data during the incubations of each Fh-OM-As material with *Desulfitobacterium* sp. DJ-3 and *Exiguobacterium* sp. DJ-4 are presented in Table S5 and are shown in Figure 2A,B. Concentrations continuously increased in all samples over the course of 18 days, and Fe(II) accounted for the vast majority of Fe_{aq}. Therefore, Fe_{aq} is referred to as $Fe(II)_{aq}$ hereafter. In Fh-As samples, $Fe(II)_{aq}$ was 0.32−0.42 mM at 18 d, while in treatments with organic adsorption complexes containing PGA and HA, $Fe(II)_{aq}$ reached to 0.45−0.58 and 0.52−0.58 mM, respectively. Thus, the microbial reductive dissolution of ferrihydrite was significantly promoted in the presence of adsorbed PGA and HA for both strains. To explore the reasons for enhanced Fe reductive dissolution in the Fh-PGA-As and Fh-HA-As samples, cell numbers of strains DJ-3 and DJ-4 at 3 d in each treatment were measured, and the results are shown in Figure 2C,D. For both the strains, cell numbers in Fh-PGA-As treatments were significantly higher than in Fh-HA-As or Fh-As treatments; the latter two being similar (Figure 2C,D). This suggests that PGA may serve as a carbon source or nutrient supplement for the strains, effectively promoting cell growth and leading to higher cell concentrations, and therefore higher rates of Fe reduction and dissolution. In control

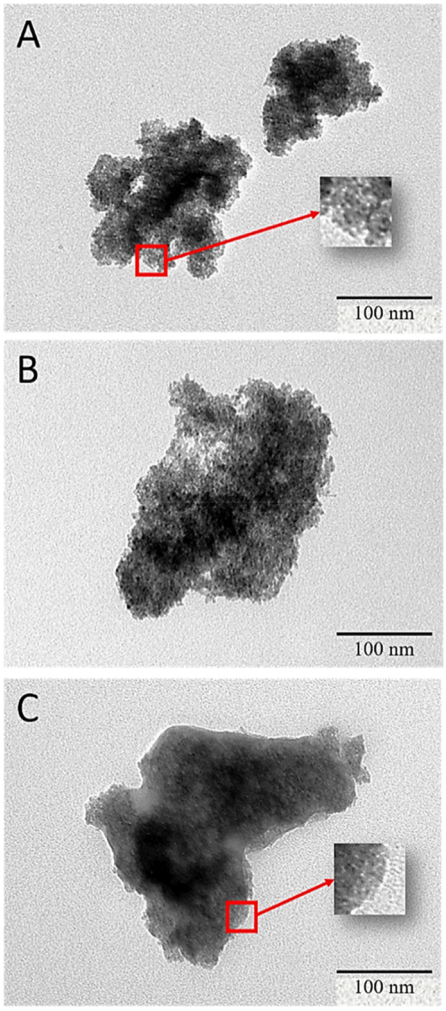

Figure 1. Transmission electron micrographs of the As(V)-adsorbed Fh and Fh-OM complexes used in this study: Fh-As (A); Fh-HA-As (B); and Fh-PGA-As (C).

treatments (without bacteria cells), $Fe(II)_{aq}$ concentrations remained below 2 μM, indicating negligible Fh dissolution by the culture medium (data not shown).

In order to eliminate the influence of cell concentration, aqueous Fe(II) concentrations were normalized by the cell numbers (Figure 2E,F). It is noteworthy that $Fe(II)_{aq}$ per cell for Fh-PGA-As was significantly lower compared to Fh-As. This suggests that the presence of PGA decreased the Fe(III) reduction rate per cell, possibly due to the blockage of interparticle pores in Fh-PGA-As (Table 1) and/or the aggregation effect of PGA (Figure 1).[12,17,18]

In contrast, the $Fe(II)_{aq}$ per cell for Fh-HA-As was higher than Fh-As, implying that the presence of HA enhanced the microbial Fe(III) reduction. This is in agreement with previous studies showing that humic acid can enhance Fe(III) reduction via an electron shuttling mechanism[17,51] with a threshold concentration of 5−10 mg dissolved C/L.[19,52] In our study, the concentration of easily desorbable carbon in Fh-HA-As was 16.3 mg/L (Table S13), which should be sufficient to enhance the Fe(III) reduction.[18] Thus, although the adsorption of HA caused a slight particle aggregation of Fh (Figure 1), the role of HA as electron shuttles overwhelmed the aggregation effect and promoted the Fe(III) reduction.

https://dx.doi.org/10.1021/acs.est.0c05329
Environ. Sci. Technol. 2021, 55, 1319−1328

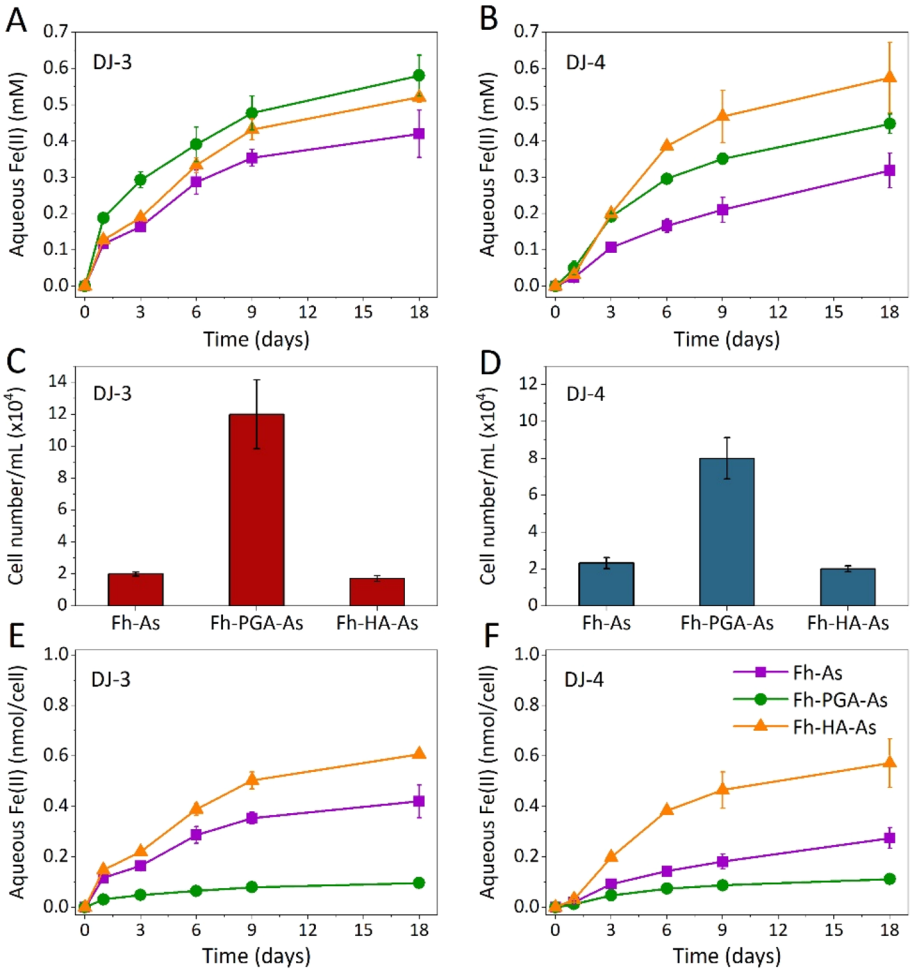

Figure 2. Aqueous Fe(II) concentrations over time during incubation of Fh-As, Fh-PGA-As, and Fh-HA-As with strain DJ-3 and DJ-4 (A, B). Cell numbers of DJ-3 and DJ-4 at 3 d in each batch (C, D). Cell numbers were measured at 3 d because pre-experiments showed that they reached a maximum at 3 d and then remained relatively stable before gradually decreasing after 9 d (data not shown). Cell normalized aqueous Fe(II) concentrations over time during incubations with DJ-3 and DJ-4 (E, F). Each data point represents the average ± standard deviation of triplicate experiments. Aqueous Fe(III) concentrations remained below 0.02 mM and are thus not shown.

Changes in Solid-Phase Fe Mineral Composition. Normalized Fe K-edge XANES spectra of (un)reacted As(V)-adsorbed Fh and Fh-OM complexes all exhibit a maximum in their first derivatives at ~7127 eV (Figure S2), implying the predominance of Fe(III) in solids. The results of principal component analysis and target-transform testing for Fe are shown in Tables S6 and S7 and Figure S3. Mineralogical composition of the solid-phase samples, evaluated by LCF of k^3-weighted Fe K-edge EXAFS spectra, are shown in Figure 3B and Table S8, and the spectra and their fits are shown in Figure 3A. After being incubated with the bacterial strains for 18 d, all samples contained small quantities of goethite (9−11%). No other secondary minerals were identified in the solid-phase. This result is consistent with previous studies demonstrating goethite dominated secondary mineral formation at lower C loadings and aqueous Fe(II) concentrations (≤1 mM).[29] The absence of crystalline peaks in the XRD patterns of the 18-day samples (Figure S4) suggests that the formed goethite was nanocrystalline. It is also possible that lepidocrocite has been an intermediate phase but was completely consumed in favor of goethite precipitation within 18 d of reaction.[29,53,54] It should also be noted that, despite the presence of phosphate in the medium (Table S3), vivianite was not identified as a secondary mineral phase.

Organic matter has been reported to complex aqueous Fe(II).[22,55] However, due to the relatively low concentrations of solid-associated OM in our experiment (C/Fe molar ratio = 0.32−0.47) and the limited Fe(II) complexation capacity of OM (at most 72 mmol Fe(II)/mol C^-),[12] the Fe(II) complexation effect of OM seemed to exert an negligible influence on the formation of goethite.

Effect of OM on Microbial As Mobilization. Aqueous As (As_{aq}) concentrations and speciation data are presented in Figure 4 and Table S10. Arsenic release was observed in all batches inoculated with bacterial strains, and all solutions contained more than 92% arsenite at 18 d. Almost no aqueous As was detected in the control treatments, demonstrating that As(III) release must be attributed to the role of Fe(III)/As(V)-reducing bacteria. As shown in Figure 4, As(III) release significantly increased for the adsorption complexes containing PGA and HA (DJ-3: Fh-PGA-As > Fh-HA-As > Fh-As; DJ-4: Fh-HA-As > Fh-PGA-As > Fh-As), which was consistent with the impact of OM on Fe(III) reduction and dissolution. A correlation analysis showed that aqueous As concentrations were significantly positive linearly correlated with Fe(II)

https://dx.doi.org/10.1021/acs.est.0c05329
Environ. Sci. Technol. 2021, 55, 1319−1328

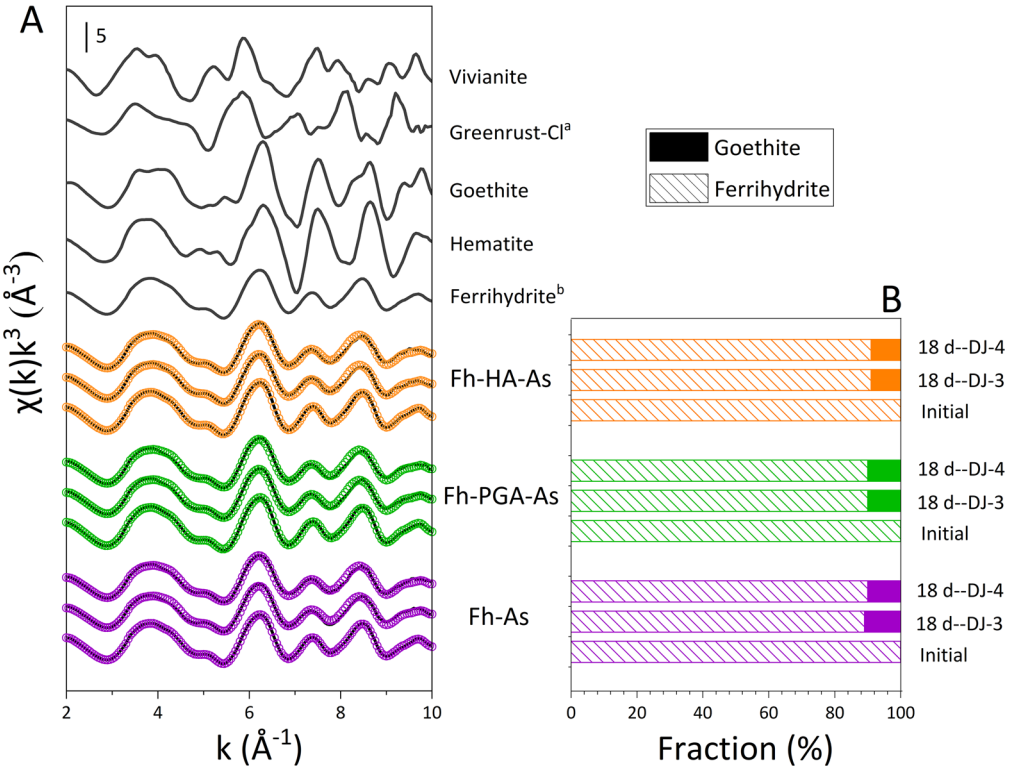

Figure 3. Fe K-edge EXAFS spectra of Fe reference compounds and linear combination fits (LCF) of (un)reacted samples (A). Data is shown as solid lines while fits are shown as open symbols. The percent fraction of each reference compound fitted in the LCF analysis (B). Fit results are presented in Table S8. [a]Spectrum courtesy of T. Borch (Colorado State University, U.S.A.). [b]Spectrum of 6-line ferrihydrite (this study).

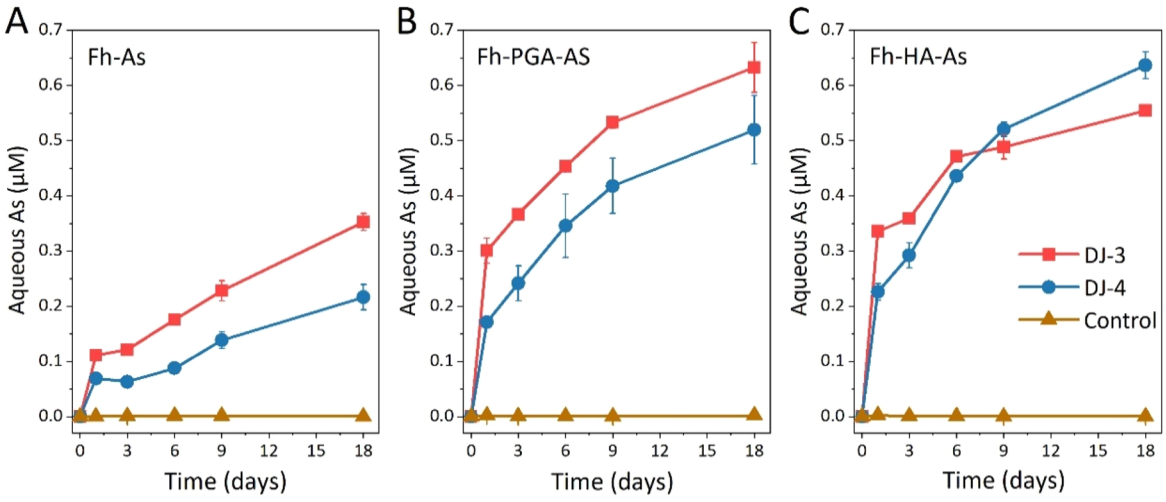

Figure 4. Aqueous As(III) concentrations over time after inoculation with strains DJ-3 and DJ-4 in the presence of Fh-As, Fh-PGA-As, and Fh-HA-As. Error bars indicate the standard deviation calculated from triplicate experiments. In all treatments, aqueous As(V) concentrations remained <0.05 μM for the duration of the experiment and no methylated As was detected. Aqueous As speciation data can be found in Table S10.

concentrations (r = 0.812, p < 0.01), indicating that the increased As release was likely a result of enhanced reductive dissolution of Fe in the adsorption complexes.[56] In As-containing samples, the molar ratio of aqueous As to Fe was $6.9–11.6 \times 10^{-4}$ at 18 d. These values are markedly lower than the molar As/Fe ratio of initial Fh-As, Fh-PGA-As, and Fh-HA-As materials ($8.6–9.3 \times 10^{-3}$, Table 1), indicating either a preferential reduction of As-free Fe sites by microorganisms, or that released As was readsorbed onto solid phase.

The latter hypothesis is strengthened by the molar ratios of aqueous As to Fe, which were slightly higher in Fh-PGA-As ($10.8–11.6 \times 10^{-4}$) and Fh-HA-As ($10.6–11.1 \times 10^{-4}$) treatments compared to Fh-As ($6.9–8.3 \times 10^{-4}$). This suggests that As readsorption may have been impeded in the OM-containing samples by the presence of OM coatings.[6,57] The adsorption of OM changes the ferrihydrite surface charge from positive to negative[13,30] and may block available ferrihydrite surface sorption sites, thereby affecting As readsorption.

Alternatively, complexation of As(III) by OM in solution may have hindered its readsorption. Multiple studies have reported that dissolved organic matter, such as HA, can complex with As(III) and form OM-As(III) complexes[58] or

https://dx.doi.org/10.1021/acs.est.0c05329
Environ. Sci. Technol. 2021, 55, 1319−1328

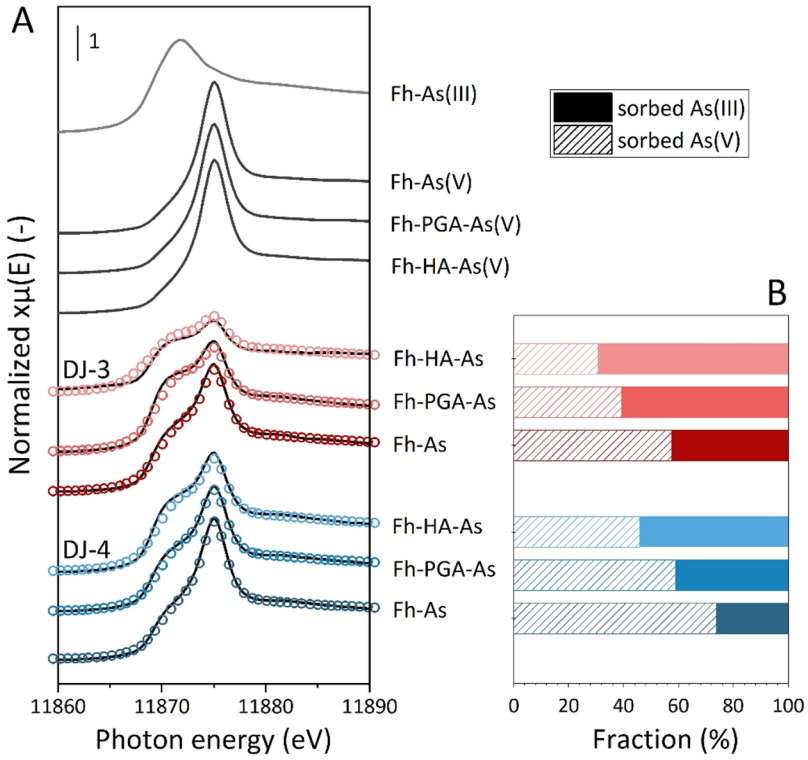

Figure 5. As K-edge XANES spectra of As reference compounds and linear combination fits (LCF) of reacted Fh-As, Fh-PGA-As, and Fh-HA-As samples (A). Data is shown as solid lines while fits are shown as open symbols. The percent fraction of each reference compound fitted in the LCF analysis (B).

OM-Fe-As(III) ternary complexes.[59] In our study, the concentration of easily desorbable OM of the Fh-HA-As was 28.9 mg/L (Table S13). In addition, previous studies showed that microbial reduction of Fh-OM complexes can also lead to the release of OM.[60,61] It seems possible that the dissolved HA may have complexed the released As(III), thus inhibiting the readsorption of As.

Contrasting Role of PGA and HA on Influencing Solid-Phase As Speciation. After being incubated with bacterial strains for 18 d, arsenic was still largely associated with the solid phase (>99%). In order to understand the effect of OM on microbial transformation of solid-phase As, XAS was employed to explore the speciation changes of mineral-associated As. The normalized As K-edge XANES spectra of all reacted samples displayed two first-derivative maxima at ∼11 869 and ∼11 874 eV (Figure S5), indicating the presence of both As(III) and As(V). Changes in the As speciation were evaluated by LCF of k^3-weighted As K-edge XANES spectra (Figure 5A), and the results are summarized in Figure 5B and Table S11. At the end of the experiment, the percentage fractions of solid-phase associated As(III) in samples Fh-As, Fh-PGA-As, and Fh-HA-As were 26−42%, 41−61%, and 54−69%, respectively (Table S11), confirming that the presence of OM significantly impacted solid-phase arsenic speciation.

Owing to its chemical composition (Figure S1), PGA cannot serve as an electron shuttle to aid in As(V) reduction. Therefore, the mechanism for increased Fe-associated As(V) reduction by PGA is likely due to its promotion of cell growth. In order to test this conjecture, an additional experiment was conducted whereby additional dissolved PGA was added to each incubation batch (Fh-As, Fh-PGA-As, and Fh-HA-As) at 0 d. After 18 days, results showed that the addition of dissolved PGA indeed lead to increased cell numbers and As(III) release in all treatments (Figure S6), thus confirming the role of PGA for the promotion of cell growth.

In contrast to PGA, HA comprises electron shuttling quinone groups.[18] A complementary additional experiment was therefore conducted to assess the impact of electron shuttles in our system, whereby additional dissolved HA was added to each incubation batch at the beginning of the experiment (0 d). Unlike PGA, the addition of dissolved HA did not result in higher cell numbers. But the concentrations of $As(III)_{aq}$ significantly increased in all treatments (Figure S6), indicating that HA similarly promoted As release. This is most likely due to the redox active electron-shuttling compounds enhancing microbial Fe(III) reductive dissolution.[18,51]

However, it must be noted that in the experiment above, the electron-shuttling effect on direct microbial As(V) reduction cannot be excluded. In order to determine whether dissolved HA could increase microbially mediated As(V) reduction rates by facilitating direct As(V) reduction through electron shuttles, a further additional experiment was conducted, whereby *Desulfitobacterium* sp. DJ-3 and *Exiguobacterium* sp. DJ-4 were incubated with soluble As(V) in the presence or absence of 50 mg/L HA. Aqueous As concentration and speciation over time during incubation is shown in Figure S7. After 36 h of incubation, the microbial reduction rates increased by 43% for strain DJ-3 and 109% for strain DJ-4 in the presence of dissolved HA. These results imply that, in our incubation experiment with adsorption complexes, the increased solid-phase As(III) fraction in Fh-HA-As samples (27−28%) was probably due to HA serving as electron shuttle to aid in direct microbial reduction of solid-phase associated As(V). This is in agreement with the high concentrations of easily desorbable OC (16.3 mg C/L$^-$) in our experiments[19,62] and previous

https://dx.doi.org/10.1021/acs.est.0c05329
Environ. Sci. Technol. 2021, 55, 1319−1328

studies showing that solid-associated humic acids can also shuttle electrons from bacteria to Fe(III) oxides.[63]

To investigate the distribution of solid-phase As (sorbed onto Fe minerals or complexed by solid-associated HA), after 18 days of microbial incubation, Fe and As concentrations were measured in Fh-HA-As samples both dissolved in concentrated HCl and digested with microwave-digestion. Since humic acids precipitate under acidic conditions at ambient temperature and pressure, dissolution with 30% HCl may only dissolve Fe-mineral-associated As. In contrast, microwave-digestion is expected to dissolve HA-associated As in addition to Fe-mineral associated As. Thus, higher As concentrations determined in the microwave-digested samples may qualitatively indicate As complexed to HA. In agreement with this, solid-phase As contents determined after microwave-digestion were 5.8−5.9 mg/g, corresponding to 92−93% of the total arsenic, while As contents determined after HCl dissolution were 3.0−3.3 mg/g, corresponding to 47−52% of the total arsenic (Table S12). Thus, it seems plausible that significant amounts of solid-phase As were bound to solid-phase humic acid.

Efficiency of Two Bacteria Strains to Utilize Electron-Shuttling Compounds. In the OM-free Fh-As batches, strain DJ-3 ultimately reduced and released 0.42 mM of Fe and 0.35 μM of As, while strain DJ-4 reduced and released 0.32 mM and 0.22 μM of Fe and As, respectively. Additionally, the LCF results show that arsenite accounted for 42−69% and 26−54% of solid-phase As after incubation with strains DJ-3 and DJ-4, respectively (Figure 5). These findings imply that *Desulfitobacterium* sp. DJ-3 is more capable of mediating the mobilization and transformation of ferrihydrite-associated Fe and As than *Exiguobacterium* sp. DJ-4.

However, the results of this study further document that the extent of Fe(III)-(oxyhydr)oxides-associated As(V) reduction and release depends not only on the As(V) reducing capacity of the microorganisms, but also on their ability to utilize electron-shuttling compounds. In the adsorption complexes containing HA, the released Fe(II) and As(III) content increased slightly (24% and 57%) with strain DJ-3 but significantly (80% and 191%) with strain DJ-4 in comparison to Fh-As samples. In the meantime, the increased percentage fraction of solid-phase arsenite in Fh-HA-As samples was also higher for strain DJ-4 than DJ-3, indicating *Exiguobacterium* sp. DJ-4, like *Shewanella putrefaciens* and *Geobacter sulfurreducens*,[19,64] could effectively utilize reduced HA to transfer electrons to Fe(III)-(oxyhydr)oxides. In the presence of HA, the concentration of aqueous As(III) in DJ-4 treatment gradually exceeded that in DJ-3 treatment (Figure 4C), indicating that the fate of Fe-associated As(V) could be significantly influenced by the strain's ability to use electron-shuttling molecules, which should be considered in future studies concerning microbially mediated solid-phase As mobilization and transformation.

■ ENVIRONMENTAL IMPLICATIONS

The results of this study indicate that PGA and HA, representing two contrasting types of OM that are commonly found in natural environments, significantly promote the microbial reduction and release of Fe(III)-(oxyhydr)oxide-associated As(V), albeit through different pathways. PGA is a major component of polysaccharide compounds found in the rhizosphere, thus the polysaccharide-promoted growth of rhizosphere microorganisms, including As(V)-reducing bacteria, could enhance the reductive dissolution of Fe-minerals and therefore the release of As. However, humic acids, which are common in sediments and wetlands, may increase As mobilization by providing electron-shuttling compounds for microbial Fe-reduction. Microbially mediated solid-phase As release was significantly promoted in the presence of PGA and HA, suggesting that the role of OM for As and Fe biogeochemical cycles in natural systems deserves greater attention.

Additionally, our study provides the first spectroscopic evidence for increased microbial solid-associated As(V) reduction in the presence of PGA and HA. The fraction of solid-associated As(III) likely increased because PGA lead to higher cell numbers and HA enhanced direct As(V)-reduction through electron shuttling mechanisms. From this point of view, microbial As(V) reduction in organic-rich soils comprising polysaccharides or humic substances may be significantly enhanced compared to in mining area soils, where organic matter content is relatively low.[65]

Collectively, this study demonstrates that polysaccharides or humic substances can result in significant variation in both As mobilization as well as solid-phase As-speciation, both of which are important to the biogeochemical cycling of soil As in redox dynamic environments. Additionally, different bacterial species showed diverse abilities to mediate Fe/As reduction and use electron-shuttling molecules, indicating that the composition of microbial soil community is a relevant factor controlling the fate of Fe-associated As(V) in organic-rich environments.

■ ASSOCIATED CONTENT

Supporting Information

The Supporting Information is available free of charge at https://pubs.acs.org/doi/10.1021/acs.est.0c05329.

Properties of the HA and PGA; experimental conditions; aqueous Fe and As concentration and speciation; solid-phase Fe and As speciation; X-ray diffraction and Fourier transform infrared (FTIR) spectroscopy data; and the effect of OM on cell growth and microbial As(V) reduction and easily desorbable OM of the adsorption complexes (PDF)

■ AUTHOR INFORMATION

Corresponding Authors

Laurel K. ThomasArrigo − *Soil Chemistry Group, Institute of Biogeochemistry and Pollutant Dynamics, Department of Environmental Systems Science, ETH Zurich, CH-8092 Zurich, Switzerland;* orcid.org/0000-0002-6758-3760; Email: laurel.thomas@usys.ethz.ch

Yanshan Cui − *College of Resources and Environment, University of Chinese Academy of Sciences, Beijing 101408, People's Republic of China;* orcid.org/0000-0002-7805-1567; Email: cuiyanshan@ucas.ac.cn

Authors

Xiaolin Cai − *College of Resources and Environment, University of Chinese Academy of Sciences, Beijing 101408, People's Republic of China; Soil Chemistry Group, Institute of Biogeochemistry and Pollutant Dynamics, Department of Environmental Systems Science, ETH Zurich, CH-8092 Zurich, Switzerland*

https://dx.doi.org/10.1021/acs.est.0c05329
Environ. Sci. Technol. 2021, 55, 1319−1328

Xu Fang − *Soil Chemistry Group, Institute of Biogeochemistry and Pollutant Dynamics, Department of Environmental Systems Science, ETH Zurich, CH-8092 Zurich, Switzerland*
Sylvain Bouchet − *Soil Chemistry Group, Institute of Biogeochemistry and Pollutant Dynamics, Department of Environmental Systems Science, ETH Zurich, CH-8092 Zurich, Switzerland;* orcid.org/0000-0002-5753-9643
Ruben Kretzschmar − *Soil Chemistry Group, Institute of Biogeochemistry and Pollutant Dynamics, Department of Environmental Systems Science, ETH Zurich, CH-8092 Zurich, Switzerland;* orcid.org/0000-0003-2587-2430

Complete contact information is available at: https://pubs.acs.org/10.1021/acs.est.0c05329

Notes

The authors declare no competing financial interest.

■ ACKNOWLEDGMENTS

We are grateful to K. Barmettler (ETH Zurich) for assisting with laboratory analyses. We thank G. Aquilanti (ELETTRA, XAFS beamline) and Dr. L. Zheng (BSRF, 1W2B beamline) for support during synchrotron measurements. The authors acknowledge the Beijing Synchrotron Radiation Facility (BSRF), the Elettra Synchrotron Light Source (ELETTRA, No. 20180024), and the Shanghai Synchrotron Radiation Facility (SSRF) for providing valuable beamtime. This work was funded by ETH Zürich and the National Natural Science Foundation of China (No. 41571451).

■ REFERENCES

(1) Bowell, R. J. Sorption of arsenic by iron-oxides and oxy-hydroxides in soils. *Appl. Geochem.* **1994**, *9* (3), 279−286.
(2) Dixit, S.; Hering, J. G. Comparison of arsenic(V) and arsenic(III) sorption onto iron oxide minerals: Implications for arsenic mobility. *Environ. Sci. Technol.* **2003**, *37* (18), 4182−4189.
(3) Guo, H.; Liu, Z.; Ding, S.; Hao, C.; Xiu, W.; Hou, W. Arsenate reduction and mobilization in the presence of indigenous aerobic bacteria obtained from high arsenic aquifers of the Hetao basin, Inner Mongolia. *Environ. Pollut.* **2015**, *203*, 50−59.
(4) Jiang, S.; Lee, J. H.; Kim, D.; Kanaly, R. A.; Kim, M. G.; Hur, H. G. Differential arsenic mobilization from As-bearing ferrihydrite by iron-respiring Shewanella strains with different arsenic-reducing activities. *Environ. Sci. Technol.* **2013**, *47* (15), 8616−8623.
(5) Ohtsuka, T.; Yamaguchi, N.; Makino, T.; Sakurai, K.; Kimura, K.; Kudo, K.; Homma, E.; Dong, D. T.; Amachi, S. Arsenic dissolution from Japanese paddy soil by a dissimilatory arsenate-reducing bacterium Geobacter sp. OR-1. *Environ. Sci. Technol.* **2013**, *47* (12), 6263−6271.
(6) Muehe, E. M.; Scheer, L.; Daus, B.; Kappler, A. Fate of arsenic during microbial reduction of biogenic versus abiogenic As-Fe(III)-mineral coprecipitates. *Environ. Sci. Technol.* **2013**, *47* (15), 8297−8307.
(7) Osborne, T. H.; McArthur, J. M.; Sikdar, P. K.; Santini, J. M. Isolation of an arsenate-respiring bacterium from a redox front in an arsenic-polluted aquifer in West Bengal, Bengal Basin. *Environ. Sci. Technol.* **2015**, *49* (7), 4193−4199.
(8) Lalonde, K.; Mucci, A.; Ouellet, A.; Gélinas, Y. Preservation of organic matter in sediments promoted by iron. *Nature* **2012**, *483* (7388), 198−200.
(9) Kögel-Knabner, I.; Guggenberger, G.; Kleber, M.; Kandeler, E.; Kalbitz, K.; Scheu, S.; Eusterhues, K.; Leinweber, P. Organo-mineral associations in temperate soils: Integrating biology, mineralogy, and organic matter chemistry. *J. Plant Nutr. Soil Sci.* **2008**, *171* (1), 61−82.
(10) Kaiser, K.; Guggenberger, G. Sorptive stabilization of organic matter by microporous goethite: sorption into small pores vs. surface complexation. *Eur. J. Soil Sci.* **2007**, *58* (1), 45−59.
(11) Schwertmann, U.; Murad, E. The nature of an iron-oxide organic iron association in a peaty environment. *Clay Miner.* **1988**, *23* (3), 291−299.
(12) Poggenburg, C.; Mikutta, R.; Schippers, A.; Dohrmann, R.; Guggenberger, G. Impact of natural organic matter coatings on the microbial reduction of iron oxides. *Geochim. Cosmochim. Acta* **2018**, *224*, 223−248.
(13) Mikutta, C.; Mikutta, R.; Bonneville, S.; Wagner, F.; Voegelin, A.; Christl, I.; Kretzschmar, R. Synthetic coprecipitates of exopolysaccharides and ferrihydrite. Part I: Characterization. *Geochim. Cosmochim. Acta* **2008**, *72* (4), 1111−1127.
(14) Mikutta, C.; Kretzschmar, R. Synthetic coprecipitates of exopolysaccharides and ferrihydrite. Part II: Siderophore-promoted dissolution. *Geochim. Cosmochim. Acta* **2008**, *72* (4), 1128−1142.
(15) Liu, H.; Li, P.; Wang, H. L.; Qing, C.; Tan, T.; Shi, B.; Zhang, G. L.; Jiang, Z.; Wang, Y. H.; Hasan, S. Z. Arsenic mobilization affected by extracellular polymeric substances (EPS) of the dissimilatory iron reducing bacteria isolated from high arsenic groundwater. *Sci. Total Environ.* **2020**, *735*, 12.
(16) Eusterhues, K.; Wagner, F. E.; Häusler, W.; Hanzlik, M.; Knicker, H.; Totsche, K. U.; Kögel-Knabner, I.; Schwertmann, U. Characterization of ferrihydrite-soil organic matter coprecipitates by X-ray diffraction and Mössbauer spectroscopy. *Environ. Sci. Technol.* **2008**, *42* (21), 7891−7897.
(17) Amstaetter, K.; Borch, T.; Kappler, A. Influence of humic acid imposed changes of ferrihydrite aggregation on microbial Fe(III) reduction. *Geochim. Cosmochim. Acta* **2012**, *85*, 326−341.
(18) Shimizu, M.; Zhou, J. H.; Schröder, C.; Obst, M.; Kappler, A.; Borch, T. Dissimilatory reduction and transformation of ferrihydrite-humic acid coprecipitates. *Environ. Sci. Technol.* **2013**, *47* (23), 13375−13384.
(19) Jiang, J.; Kappler, A. Kinetics of microbial and chemical reduction of humic substances: Implications for electron shuttling. *Environ. Sci. Technol.* **2008**, *42* (10), 3563−3569.
(20) Lovley, D. R.; Coates, J. D.; Blunt-Harris, E. L.; Phillips, E. J. P.; Woodward, J. C. Humic substances as electron acceptors for microbial respiration. *Nature* **1996**, *382* (6590), 445−448.
(21) Cooper, R. E.; Eusterhues, K.; Wegner, C. E.; Totsche, K. U.; Küsel, K. Ferrihydrite-associated organic matter (OM) stimulates reduction by Shewanella oneidensis MR-1 and a complex microbial consortia. *Biogeosciences* **2017**, *14* (22), 5171−5188.
(22) Royer, R. A.; Burgos, W. D.; Fisher, A. S.; Unz, R. F.; Dempsey, B. A. Enhancement of biological reduction of hematite by electron shuttling and Fe(II) complexation. *Environ. Sci. Technol.* **2002**, *36* (9), 1939−1946.
(23) Jones, A. M.; Collins, R. N.; Rose, J.; Waite, T. D. The effect of silica and natural organic matter on the Fe(II)-catalysed transformation and reactivity of Fe(III) minerals. *Geochim. Cosmochim. Acta* **2009**, *73* (15), 4409−4422.
(24) Hu, S.; Lu, Y.; Peng, L.; Wang, P.; Zhu, M.; Dohnalkova, A. C.; Chen, H.; Lin, Z.; Dang, Z.; Shi, Z. Coupled kinetics of ferrihydrite transformation and As(V) sequestration under the effect of humic acids: A mechanistic and quantitative study. *Environ. Sci. Technol.* **2018**, *52* (20), 11632−11641.
(25) Zachara, J. M.; Kukkadapu, R. K.; Peretyazhko, T.; Bowden, M.; Wang, C.; Kennedy, D. W.; Moore, D.; Arey, B. The mineralogic transformation of ferrihydrite induced by heterogeneous reaction with bioreduced anthraquinone disulfonate (AQDS) and the role of phosphate. *Geochim. Cosmochim. Acta* **2011**, *75* (21), 6330−6349.
(26) Chen, Z.; Wang, Y.; Jiang, X.; Fu, D.; Xia, D.; Wang, H.; Dong, G.; Li, Q. Dual roles of AQDS as electron shuttles for microbes and dissolved organic matter involved in arsenic and iron mobilization in the arsenic-rich sediment. *Sci. Total Environ.* **2017**, *574*, 1684−1694.
(27) Chan, C. S.; De Stasio, G.; Welch, S. A.; Girasole, M.; Frazer, B. H.; Nesterova, M. V.; Fakra, S.; Banfield, J. F. Microbial

polysaccharides template assembly of nanocrystal fibers. *Science* **2004**, *303* (5664), 1656−1658.
(28) Emerson, D.; Weiss, J. V.; Megonigal, J. P. Iron-oxidizing bacteria are associated with ferric hydroxide precipitates (Fe-plaque) on the roots of wetland plants. *Appl. Environ. Microbiol.* **1999**, *65* (6), 2758−2761.
(29) ThomasArrigo, L. K.; Byrne, J. M.; Kappler, A.; Kretzschmar, R. Impact of organic matter on iron(II)-catalyzed mineral transformations in ferrihydrite-organic matter coprecipitates. *Environ. Sci. Technol.* **2018**, *52* (21), 12316−12326.
(30) ThomasArrigo, L. K.; Kaegi, R.; Kretzschmar, R. Ferrihydrite growth and transformation in the presence of ferrous iron and model organic ligands. *Environ. Sci. Technol.* **2019**, *53* (23), 13636−13647.
(31) Kauri, T. Fluctuations in physiological groups of bacteria in the horizons of a beech forest soil. *Soil Biol. Biochem.* **1983**, *15* (1), 45−50.
(32) Vancura, V.; Kunc, F. *Soil Microbial Associations: Control of Structures and Functions*; Elsevier: Amsterdam, Netherlands, 1988.
(33) Cai, X.; Zhang, Z.; Yin, N.; Du, H.; Li, Z.; Cui, Y. Comparison of arsenate reduction and release by three As(V)-reducing bacteria isolated from arsenic-contaminated soil of Inner Mongolia, China. *Chemosphere* **2016**, *161*, 200−207.
(34) Cai, X.; Wang, P.; Li, Z.; Li, Y.; Yin, N.; Du, H.; Cui, Y. Mobilization and transformation of arsenic from ternary complex OM-Fe(III)-As(V) in the presence of As(V)-reducing bacteria. *J. Hazard. Mater.* **2020**, *381*, 120975.
(35) Niggemyer, A.; Spring, S.; Stackebrandt, E.; Rosenzweig, R. F. Isolation and characterization of a novel As(V)-reducing bacterium: Implications for arsenic mobilization and the genus Desulfitobacterium. *Appl. Environ. Microbiol.* **2001**, *67* (12), 5568−5580.
(36) Villemur, R.; Lanthier, M.; Beaudet, R.; Lépine, F. The Desulfitobacterium genus. *FEMS Microbiol. Rev.* **2006**, *30* (5), 706−733.
(37) Yamamura, S.; Sudo, T.; Watanabe, M.; Tsuboi, S.; Soda, S.; Ike, M.; Amachi, S. Effect of extracellular electron shuttles on arsenic-mobilizing activities in soil microbial communities. *J. Hazard. Mater.* **2018**, *342*, 571−578.
(38) Knee, E. M.; Gong, F. C.; Gao, M. S.; Teplitski, M.; Jones, A. R.; Foxworthy, A.; Mort, A. J.; Bauer, W. D. Root mucilage from pea and its utilization by rhizosphere bacteria as a sole carbon source. *Mol. Plant-Microbe Interact.* **2001**, *14* (6), 775−784.
(39) Schwertmann, U.; Cornell, R. M. *Iron Oxides in the Laboratory: Preparation and Characterization*; Wiley-VCH: Weinheim, Germany, 2000.
(40) Hofmann, A.; Pelletier, M.; Michot, L.; Stradner, A.; Schurtenberger, P.; Kretzschmar, R. Characterization of the pores in hydrous ferric oxide aggregates formed by freezing and thawing. *J. Colloid Interface Sci.* **2004**, *271* (1), 163−173.
(41) Raber, G.; Stock, N.; Hanel, P.; Murko, M.; Navratilova, J.; Francesconi, K. A. An improved HPLC-ICPMS method for determining inorganic arsenic in food: Application to rice, wheat and tuna fish. *Food Chem.* **2012**, *134* (1), 524−532.
(42) Fortune, W. B.; Mellon, M. G. Determination of iron with o-phenanthroline - A spectrophotometric study. *Ind. Eng. Chem., Anal. Ed.* **1938**, *10*, 60−64.
(43) Brunauer, S.; Emmett, P. H.; Teller, E. Adsorption of gases in multimolecular layers. *J. Am. Chem. Soc.* **1938**, *60*, 309−319.
(44) Barrett, E. P.; Joyner, L. G.; Halenda, P. P. The determination of pore volume and area distributions in porous substances. I. Computations from nitrogen isotherms. *J. Am. Chem. Soc.* **1951**, *73* (1), 373−380.
(45) Ravel, B.; Newville, M. ATHENA, ARTEMIS, HEPHAESTUS: data analysis for X-ray absorption spectroscopy using IFEFFIT. *J. Synchrotron Radiat.* **2005**, *12*, 537−541.
(46) Webb, S. M. SIXPack: a graphical user interface for XAS analysis using IFEFFIT. *Phys. Scr.* **2005**, *T115*, 1011−1014.
(47) Yin, N. Y.; Zhang, Z. N.; Cai, X. L.; Du, H. L.; Sun, G. X.; Cui, Y. S. In vitro method to assess soil arsenic metabolism by human gut microbiota: Arsenic speciation and distribution. *Environ. Sci. Technol.* **2015**, *49* (17), 10675−10681.
(48) Liu, C.; Huang, P. M. Kinetics of lead adsorption by iron oxides formed under the influence of citrate. *Geochim. Cosmochim. Acta* **2003**, *67* (5), 1045−1054.
(49) Kaiser, K.; Guggenberger, G. Mineral surfaces and soil organic matter. *Eur. J. Soil Sci.* **2003**, *54* (2), 219−236.
(50) Schwertmann, U.; Friedl, J.; Stanjek, H. From Fe(III) ions to ferrihydrite and then to hematite. *J. Colloid Interface Sci.* **1999**, *209* (1), 215−223.
(51) Kappler, A.; Benz, M.; Schink, B.; Brune, A. Electron shuttling via humic acids in microbial iron(III) reduction in a freshwater sediment. *FEMS Microbiol. Ecol.* **2004**, *47* (1), 85−92.
(52) O'Loughlin, E. J.; Gorski, C. A.; Scherer, M. M.; Boyanov, M. I.; Kemner, K. M. Effects of oxyanions, natural organic matter, and bacterial cell numbers on the bioreduction of lepidocrocite (γ-FeOOH) and the formation of secondary mineralization products. *Environ. Sci. Technol.* **2010**, *44* (12), 4570−4576.
(53) Hansel, C. M.; Benner, S. G.; Fendorf, S. Competing Fe(II)-induced mineralization pathways of ferrihydrite. *Environ. Sci. Technol.* **2005**, *39* (18), 7147−7153.
(54) Boland, D. D.; Collins, R. N.; Miller, C. J.; Glover, C. J.; Waite, T. D. Effect of solution and solid-phase conditions on the Fe(II)-accelerated transformation of ferrihydrite to lepidocrocite and goethite. *Environ. Sci. Technol.* **2014**, *48* (10), 5477−5485.
(55) Royer, R. A.; Burgos, W. D.; Fisher, A. S.; Jeon, B. H.; Unz, R. F.; Dempsey, B. A. Enhancement of hematite bioreduction by natural organic matter. *Environ. Sci. Technol.* **2002**, *36* (13), 2897−2904.
(56) Islam, F. S.; Gault, A. G.; Boothman, C.; Polya, D. A.; Charnock, J. M.; Chatterjee, D.; Lloyd, J. R. Role of metal-reducing bacteria in arsenic release from Bengal delta sediments. *Nature* **2004**, *430* (6995), 68−71.
(57) Kleinert, S.; Muehe, E. M.; Posth, N. R.; Dippon, U.; Daus, B.; Kappler, A. Biogenic Fe(III) minerals lower the efficiency of iron-mineral-based commercial filter systems for arsenic removal. *Environ. Sci. Technol.* **2011**, *45* (17), 7533−7541.
(58) Buschmann, J.; Kappeler, A.; Lindauer, U.; Kistler, D.; Berg, M.; Sigg, L. Arsenite and arsenate binding to dissolved humic acids: Influence of pH, type of humic acid, and aluminum. *Environ. Sci. Technol.* **2006**, *40* (19), 6015−6020.
(59) Hoffmann, M.; Mikutta, C.; Kretzschmar, R. Arsenite binding to natural organic matter: Spectroscopic evidence for ligand exchange and ternary complex formation. *Environ. Sci. Technol.* **2013**, *47* (21), 12165−12173.
(60) Adhikari, D.; Zhao, Q.; Das, K.; Mejia, J.; Huang, R. X.; Wang, X. L.; Poulson, S. R.; Tang, Y. Z.; Roden, E. E.; Yang, Y. Dynamics of ferrihydrite-bound organic carbon during microbial Fe reduction. *Geochim. Cosmochim. Acta* **2017**, *212*, 221−233.
(61) Pan, W.; Kan, J.; Inamdar, S.; Chen, C.; Sparks, D. Dissimilatory microbial iron reduction release DOC (dissolved organic carbon) from carbon-ferrihydrite association. *Soil Biol. Biochem.* **2016**, *103*, 232−240.
(62) Piepenbrock, A.; Dippon, U.; Porsch, K.; Appel, E.; Kappler, A. Dependence of microbial magnetite formation on humic substance and ferrihydrite concentrations. *Geochim. Cosmochim. Acta* **2011**, *75* (22), 6844−6858.
(63) Roden, E. E.; Kappler, A.; Bauer, I.; Jiang, J.; Paul, A.; Stoesser, R.; Konishi, H.; Xu, H. Extracellular electron transfer through microbial reduction of solid-phase humic substances. *Nat. Geosci.* **2010**, *3* (6), 417−421.
(64) Poggenburg, C.; Mikutta, R.; Sander, M.; Schippers, A.; Marchanka, A.; Dohrmann, R.; Guggenberger, G. Microbial reduction of ferrihydrite-organic matter coprecipitates by Shewanella putrefaciens and Geobacter metallireducens in comparison to mediated electrochemical reduction. *Chem. Geol.* **2016**, *447*, 133−147.
(65) Shrestha, R. K.; Lal, R. Changes in physical and chemical properties of soil after surface mining and reclamation. *Geoderma* **2011**, *161* (3−4), 168−176.

https://dx.doi.org/10.1021/acs.est.0c05329
Environ. Sci. Technol. 2021, 55, 1319−1328